

Technical Notes

TECHNICAL NOTES are short manuscripts describing new developments or important results of a preliminary nature. These Notes cannot exceed 6 manuscript pages and 3 figures; a page of text may be substituted for a figure and vice versa. After informal review by the editors, they may be published within a few months of the date of receipt. Style requirements are the same as for regular contributions (see inside back cover).

Trajectory Integration in Vortical Flows

Earl M. Murman* and Kenneth G. Powell†
Massachusetts Institute of Technology,
Cambridge, Massachusetts

Introduction

THE use of streamlines or particle traces can be very helpful in understanding the complicated flow patterns that result from vortical flows.¹⁻⁴ Such traces represent a trajectory integration through a given velocity field. For our interests, the velocity field is created from a computational simulation, but it also could result from experimental measurements. Trajectory integrations can be subject to numerical error. Results are presented that show the effect of step size and order of accuracy of the integration method on the computation of vortical streamlines. A paper recently presented by the authors⁵ contained erroneous results regarding streamline topologies for vortical flows. Corrected results using a more accurate streamline integration are given here.

Model Problem

In order to assess the accuracy of different trajectory calculations, a model set of equations is selected that has the characteristics of a vortical flow. The hypothetical velocity field

$$u = \frac{dx}{dt} = ax - by \quad (1a)$$

$$v = \frac{dy}{dt} = ay + bx \quad (1b)$$

produces particle trajectories given by

$$x(t) = \exp(at)[x_0 \cos bt - y_0 \sin bt] \quad (2a)$$

$$y(t) = \exp(at)[x_0 \sin bt + y_0 \cos bt] \quad (2b)$$

where t represents the distance along a trajectory. The model is similar to a two-dimensional vortex of strength $2\pi b$ and a source of strength $2\pi a$ superposed at the origin, but without the singular $1/r$ effect in the velocity field. The above solution with $a = -1/2$ and $b = 3$ is shown in Fig. 1 for the domain ($|x| \leq 1$, $|y| \leq 1$).

Numerical Integration

A trajectory integration scheme described below has been tried for the model problem using both a first-order-accurate

forward Euler and a second-order-accurate predictor-corrector method. The calculations were done on a 25×25 rectangular grid. It is assumed that discrete data are given for the u, v velocity field at the nodes of the quadrilateral grid. Since velocity components are needed at arbitrary points within each cell, bilinear interpolation

$$u(x, y) = (a_1 + b_1 x)(c_1 + d_1 y) \\ = a_1 c_1 + b_1 c_1 x + a_1 d_1 y + b_1 d_1 xy \quad (3a)$$

$$v(x, y) = (a_2 + b_2 x)(c_2 + d_2 y) \\ = a_2 c_2 + b_2 c_2 x + a_2 d_2 y + b_2 d_2 xy \quad (3b)$$

is used, where a, b, c, d are determined from the values at the four corner points. (For a general nonorthogonal curvilinear coordinate system, an isoparametric mapping is done from physical x, y to computational ξ, η where the bilinear interpolation is applied.) It can be seen that the bilinear interpolation formula creates a nonlinear function definition due to the cross product xy . Thus, a step size smaller than the cell size must be used for the trajectory to follow the local velocity direction, particularly in a region of rapid variation such as the spiral of Fig. 1.

The integration is carried out using the parametric equations

$$dx = u dt, \quad dy = v dt \quad (4)$$

Starting at a point, a line segment is drawn to a predicted point a fraction $\Delta s = \bar{U} \Delta t$ of the cell width, where $\bar{U} = \max(u, v)$ of the four corner values. With no correction step, a forward Euler method results. For $\Delta s = 1$, the results are shown in Fig. 2a. It can be seen that a limit line is reached, and the spiral singularity is not resolved. For $\Delta s = 0.1$, the limit line shrinks to that shown in Fig. 2b. For the predictor-corrector versions, the bilinear interpolation is used at the new point to obtain predicted values of u, v , which are averaged with the initial values to obtain a corrected position. Results for this are shown in Figs. 2c ($\Delta s = 1.0$) and 2d ($\Delta s = 0.1$). For the larger step size, an erratic behavior near the origin results, because

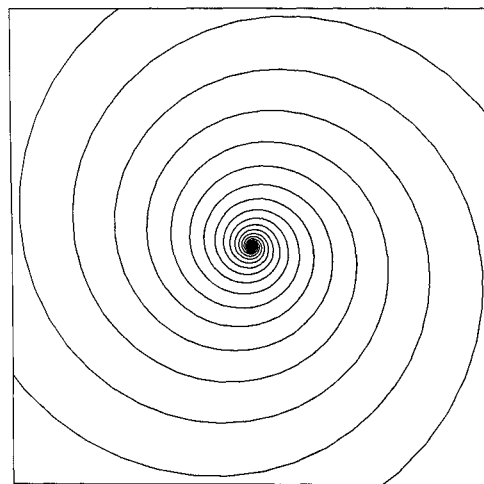


Fig. 1 Exact solution for particle trajectories given by Eq. (2).

Received July 14, 1987; revision received June 28, 1988. Copyright © 1988 American Institute of Aeronautics and Astronautics, Inc. All rights reserved.

*Professor, Department of Aeronautics and Astronautics. AIAA Fellow.

†Research Assistant, Department of Aeronautics and Astronautics; currently Assistant Professor, Department of Aerospace Engineering, University of Michigan, Ann Arbor, Michigan. AIAA Member.

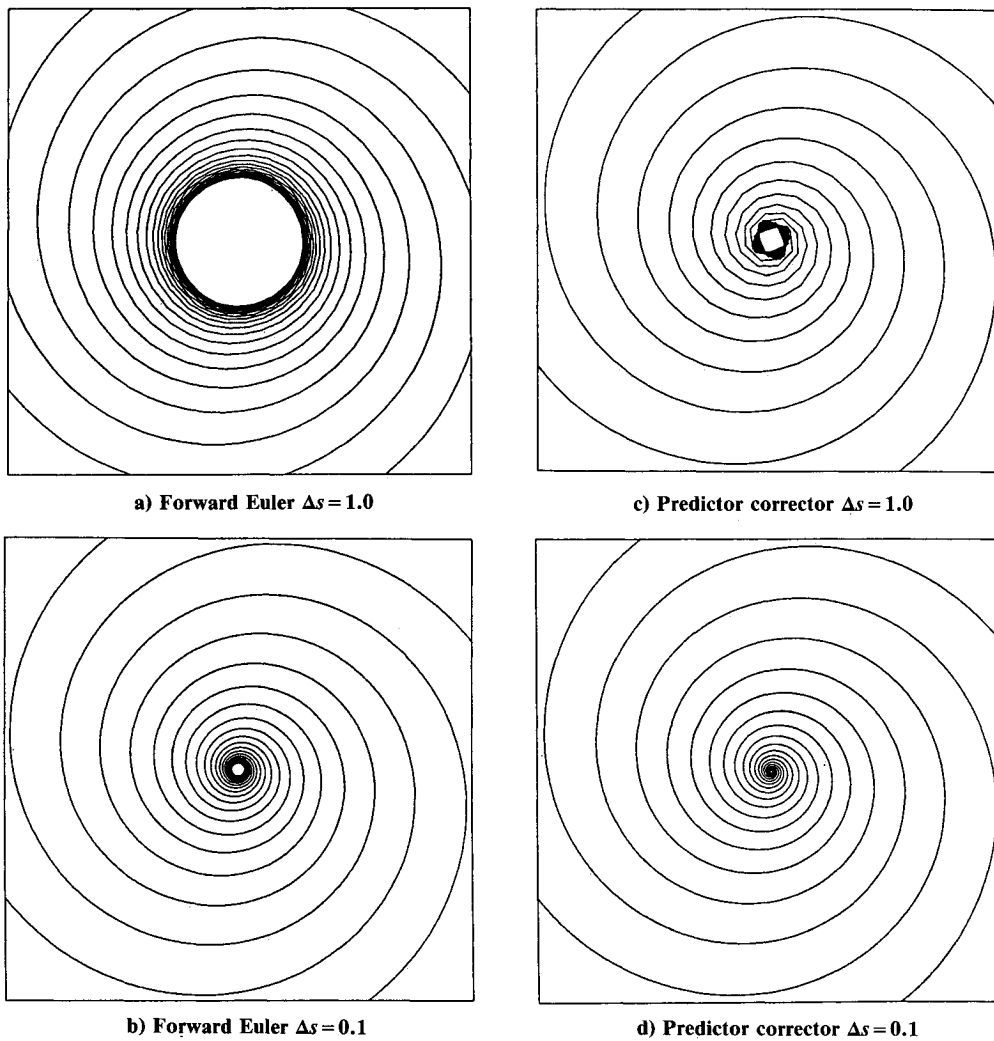
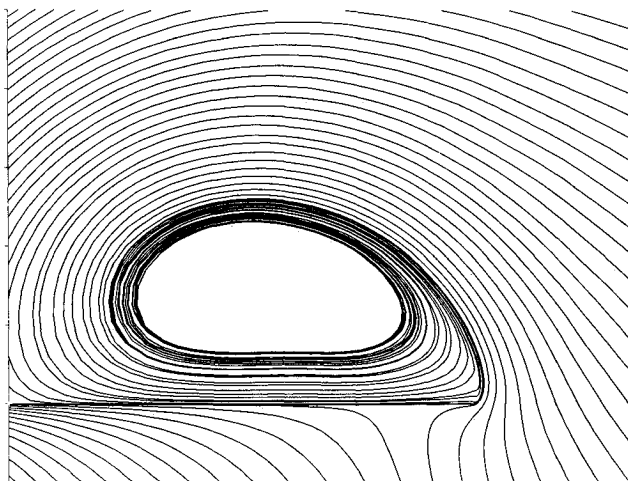


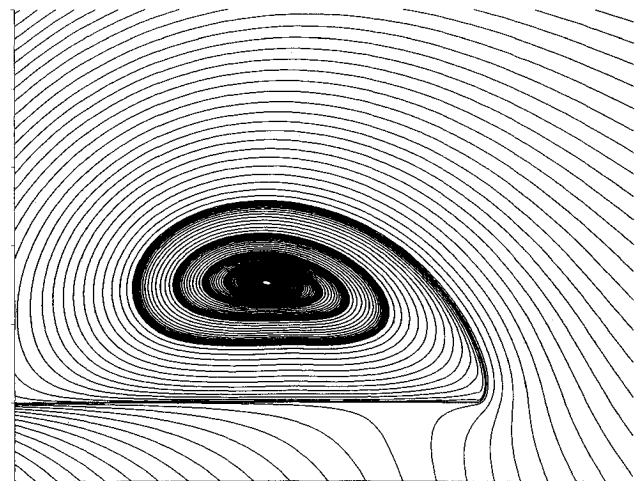
Fig. 2 Particle trajectories.

Fig. 3 Conical streamlines for leading-edge vortex on a 75-deg swept flat plate delta wing, $\alpha = 10$ deg, $M_\infty = 1.3$ —forward Euler $\Delta s = 1.0$.

the velocity directions change drastically across the cell. For step sizes a fraction of the cell size, acceptable results are obtained with the predictor-corrector, and they agree quite well with the exact solution (Fig. 1).

Conical Streamlines

A number of papers by the authors has displayed the limiting line behavior. This was a result of using a streamline

Fig. 4 Conical streamlines for leading-edge vortex on a 75-deg swept flat plate delta wing, $\alpha = 10$ deg, $M_\infty = 1.3$ —predictor-corrector $\Delta s = 0.2$.

integrator with a step size on the order of the cell size. To avoid the erratic behavior near the center of the vortex, the streamline integrator reverted to first order in that region. Typical results using this approach for conical streamlines of a leading-edge vortex generated by a flat plate delta wing with 75-deg leading-edge sweep at 10-deg angle of attack in a $M_\infty = 1.3$ freestream are shown in Fig. 3. The results corre-

spond to those presented in Ref. 5 wherein it was reported that the vortex had a limiting line within which the streamlines spiraled outward from the vortex center. Conical streamlines for the same velocity field using a predictor-corrector method with a step size of $\Delta s = 0.2$ are shown in Fig. 4. It can be seen that the streamlines spiral inward to the center with a small void on the order of the step size. However, for some flow conditions, even using the predictor-corrector method with $\Delta s = 0.001$ is not sufficient to obtain the spiral trajectory.⁴ For these cases, the radial velocity into the vortex center is just too small compared to the circumferential velocity.

Conclusions

The importance of step size and order of accuracy of the streamline integration is demonstrated for a model problem representing vortical flow. Results for a conical vortex show the correct expected behavior when the more accurate method is used, in contrast to erroneous results reported earlier.⁵

Acknowledgments

This work was supported by the Office of Naval Research under Grant N00014-86-K-0288, monitored by Dr. Spiro Lekoudis.

References

- ¹Marconi, F., "The Spiral Singularity in the Supersonic Inviscid Flow over a Cone," AIAA Paper 83-1665, July 1983.
- ²Murman, E., Rizzi, A., and Powell, K., "High Resolution Solutions of the Euler Equations for Vortex Flows," *Progress and Supercomputing in Computational Fluid Dynamics*, Birkhauser-Boston, Boston, MA, 1985, pp. 93-113.
- ³Lasinski, T., Buning, P., Choi, D., Rogers, S., Bancroft, G., and Merritt, F., "Flow Visualization of CFD Using Graphics Workstations," AIAA Paper 87-1180CP, June 1987.
- ⁴Powell, K. G., "Vortical Solutions of the Conical Euler Equations," Ph.D. Thesis, Massachusetts Inst. of Technology, Dept. of Aeronautics and Astronautics, Cambridge, MA, July 1987.
- ⁵Murman, E. M., Powell, K. G., Goodsell, A. M., and Landahl, M., "Leading-Edge Vortex Solutions with Large Total Pressure Losses," AIAA Paper 87-0039, Jan. 1987.

Skin-Friction Measurements by Laser-Beam Interferometry

U. R. Müller* and F. Feyzi†

Aerodynamisches Institut,
Rheinisch-Westfälische Technische Hochschule,
Aachen, Federal Republic of Germany

Introduction

SOPHISTICATED methods for measuring the wall shear stress in complex turbulent flows have been developed in recent years, notably the floating-element technique,¹ the pulsed-wire technique,² and the oil film laser interferometer of

Monson.³ The applicability of the techniques quoted is not limited to flows with near-wall similarity of the mean velocity profile, which is required for standard techniques such as the Preston tube or Clauser chart that infer the skin friction from measured velocities. In this Note, a modified version of the laser interferometer method is reported as well as its experimental validation and application in two-dimensional, incompressible, turbulent boundary layers.

Measuring Technique

The laser interferometer technique records the changing thickness with time of a thin oil film (less than $25\mu\text{m}$) that has been applied to the wall surface at the measuring position and experiences the shear stress of the external stream. Monson's method employs two laser beams, which are generated by an interferometer flat and focused on the wall (Fig. 1a). Each beam is partly reflected at both the surface of the oil film and the wall, thereby generating interference patterns. By means of suitable receiving optics, both reflected interfering beams are focused on photodiodes, which monitor the time change of the intensities; an example of the fringe time records is given in Fig. 1b. Each crest interval corresponds to a change in oil-film thickness by one laser wavelength.

In the present work, two modifications have been introduced into Monson's measuring system. Our experiments were performed at a much larger focal length (1 m) than the one used in Ref. 3. As a consequence, the intensity of the beams reflected from the polished aluminum plate, which was used as a wall surface, proved to be rather weak and yielded noisy fringe time records. We succeeded in improving the quality of the records (see Fig. 1b) by coating the wall with a thin transparent plastic foil sprayed black on the back side. This increased the beam intensity by a factor of three. Furthermore, we developed substantially simplified receiving optics, which replaced the more complex beam splitter of Ref. 3; we

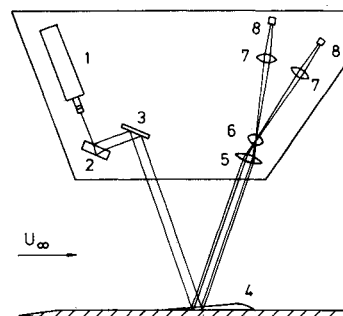


Fig. 1a Schematic of dual-laser-beam skin-friction interferometer: 1) He-Ne-laser with telescope; 2) interferometer flat; 3) mirror; 4) oil film; 5, 6, 7) biconvex lenses; 8) photodiodes.

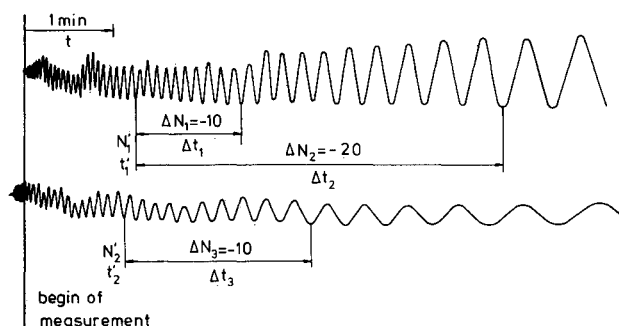


Fig. 1b Measured interferometer fringe time records, beam spacing 5 mm; upper part: downstream beam.

Received May 10, 1988; revision received June 29, 1988. Copyright © 1988 American Institute of Aeronautics and Astronautics, Inc. All rights reserved.

*Research Scientist, Messerschmitt-Bölkow-Blohm GmbH, Bremen, FRG.

†Research Scientist.